Malaysian Journal of Chemistry, 2026, Vol. 28(1), 490-500
(Special Issue: *12th International Conference of the College of Science & 3rd Conference of Chemistry Department 2025*)

Design, Synthesis, and Molecular Docking Studies of New Pyrazole Derivatives as Potent Antimicrobial Agents Targeting ALDH9A1

Helen Abd Alhassan Mahmood[1]*, Yasir Mohamed Kadhim[2], Nabel Bunyan Ayrim[3] and Fadhel Rukhis Hafedh[3]
[1]Department of Applied Chemistry, College of Applied Science, University of Fallujah, Anbar, Iraq
[2]Department of Pharmaceutical Chemistry, College of Pharmacy, Al-Nahrain University, Baghdad, Iraq
[3]Department of Chemistry, College of Science, Mustansiriyah University, Baghdad, Iraq
*Corresponding author (e-mail: helen.abdulhassan@uofallujah.edu.iq)

This study presents the synthesis and characterization of a series of pyrazole derivatives [**H5-H8**] incorporating a furan moiety, using FT-IR, ^{1}H NMR, ^{13}C NMR, and elemental analysis. The initial phase involved the reaction of 4-aminoacetophenone with various substituted aromatic aldehydes in absolute ethanol at room temperature, yielding α,β-unsaturated carbonyls [**H1-H4**]. Subsequent treatment with hydrazine hydrate in glacial acetic acid yielded the pyrazole derivatives [**H 5-H8**]. The antimicrobial efficacy of the synthetic compounds was evaluated against both gram-positive bacteria (Staphylococcus aureus and Staphylococcus epidermis) and two gram-negative bacteria (Escherichia coli and Klebsiella sp.), whereas the antifungal activity has been examined against Candida albicans. The results revealed that most synthetic pyrazole derivatives exhibit a significant percentage of antimicrobial activity relative to the reference antibiotic ampicillin. The synthesized derivatives [**H5-H8]** underwent evaluation via docking of molecules, employing optimization of genetics within the docking suite for ligands, and the ADME studies showed that all compounds fulfilled the Lipinski rule to assess their antioxidant activity against the enzyme Aldehyde dehydrogenase 9A1 (ALDH9A1), a human enzyme that catalyzes the oxidation of NAD+.

Keywords: Pyrazole, antimicrobial activity, Docking study, ADME

Received: October 2025; Accepted: October 2025

Chalcones are a kind of flavonoid. For open-chain flavonoids, the carbonyl groups of α, β-unsaturated or saturated carbons link two aromatic rings, the Claisen-Schmidt condensation that serves for chalcone synthesis [1]. In the plant kingdom, this is regarded as one of the most significant categories of natural products. A catalyst or condensing agent is often needed to create chalcones by condensing aryl ketones with aromatic aldehydes [2]. Numerous heterocyclic processes have employed chalcone compounds to yield a range of biologically active molecules that serve as therapeutic targets [3]. The synthesized molecules demonstrated analgesic, anti-arthritis, anti-inflammatory, antimalarial, antipyretic, anti-bacterial, antiviral, and anticancer effects [4–6]. Many investigations have demonstrated that chalcones exhibit anti-proliferative and cytotoxic properties [7]. Subsequently, they underwent structural modification by the production of various polyfunctionally substituted compounds [8]. The elimination of the α, β-unsaturated carbonyl system has been demonstrated to reduce their biological activity [9]. Various synthetic alterations, including biphenyl-containing fused heterocyclic molecules [10] and chalcones derived from coumarins [11], as well as other substitutions, were documented to influence the biological activity, such as the anticancer properties, of chalcones [12]. For this study, due to the significant medicinal properties of chalcones previously mentioned, researchers aimed to conduct various hetero cyclization processes of certain chalcones, resulting in the synthesis of pyrazole rings [13, 14]. The basic structures of many biologically active molecules are nitrogen-containing heterocyclic compounds, which have many uses, especially in medical chemistry and biology. Pyrazoles are recognized aromatic heterocyclic compounds characterized by two atoms of nitrogen. Within the ring are five members, and they are found in various natural and manufactured bioactive compounds [15]. Significantly, derivatives of pyrazoles constitute a crucial class of chemicals exhibiting a broad range of biological activities [16]. Differing modifications may be required to achieve prospective effects through bacterial and fungal infections that are resistant to multiple drugs. The widespread misuse and inadequate patient compliance are responsible for growing bacterial resistance to current treatments, which are quickly reaching concerning proportions. A significant crisis in the health of infections has just emerged, in conjunction with the decrease in the rate of antibiotic discovery [17, 18].

†Paper presented at the 12th International Conference of the College of Science & 3rd Conference of Chemistry Dept. 2025

Consequently, it is essential to investigate different antibacterial agent classes that have appropriate pharmacokinetic, toxicological, and therapeutic properties. [19]. Various drug molecules featuring pyrazole and pyrazoline rings with diverse activities are presently available in the market. Celecoxib, fezolamine, and tepoxalin are adducible in Figure 1 [20].

Many biological actions, including antibacterial, antifungal, antiviral, analgesic, antidepressant, anti-inflammatory, and anticancer properties, are exhibited by pyrazolines. [21–24]. Once many of the properties of the molecules can be computed in advance, silico predictions can help with this procedure by lowering the number of molecules synthesized and evaluated. The existing models and methods can forecast metabolism, distribution, absorption, and structure-based in silico tools, such as molecular docking, which can forecast potential interactions with the study target [25–27].

Recently, researchers have been looking into pyrazole as a pharmacophore for making possible antioxidants. This work has led to the creation of various molecules that have pyrazole cores in their structures. Here are some of the synthetic series of pyrazoles that have been reported: N-(4-(1-acetyl-5-(5-(sub-phenyl) furan-2-yl) 4,5-dihydro-1H-pyrazol-3-yl) phenyl) acetamide had strong radical scavenging excretion, toxicity (ADMET), and activity (RSA) against 2,2-diphenyl-1-picrylhydrazyl (DPPH) radical. The results suggest that it could be an effective antibacterial and antifungal agent.

EXPERIMENTAL SECTION

Materials

All used compounds were *p*-amino acetophenon, *p*-choro-furan-2-carbaldehyde, *p*-nitro-furan-2-carbaldehyde, 2,4-dichloro-furan-2-carbaldehyde, *p*-bromo-furan-2-carbaldehyde, and Hydrazine hydrate from Sigma Aldrich. The reagents and solvents sodium hydroxide, glacial acetic acid, hydrochloric acid, and ethanol absolute were purchased from Sigma Aldrich.

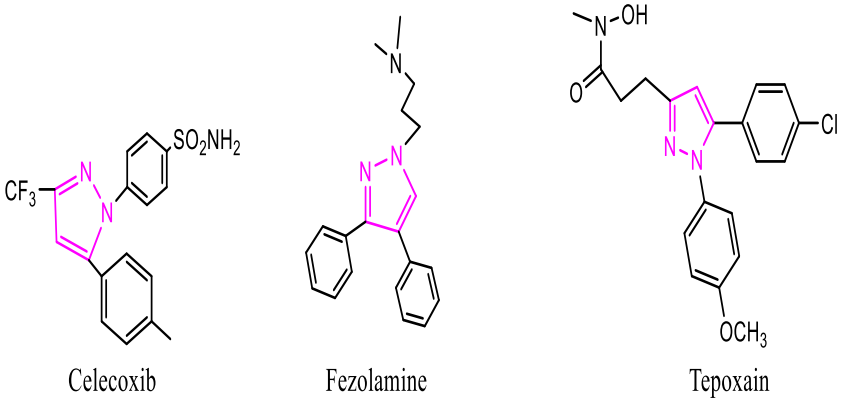

Figure 1. The chemical composition of pyrazole derivatives.

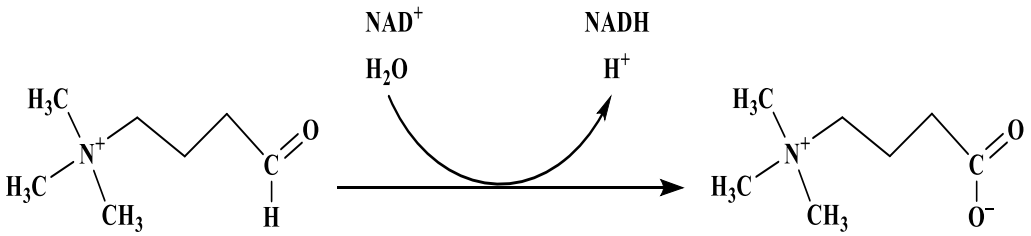

Figure 2. Reaction catalyzed by ALDH9A1.

Instrumentation

The melting points of the synthesized chalcone and pyrazole compounds were measured and uncorrected in an open capillary tube using a Gallen Kamp MFB-600 melting point equipment. Thin-layer chromatography (TLC) with eluents of n-hexane: ethyl acetate was used to observe the TLC spots that formed during the reactions in this work. Using a Shimadzu FT-IR-8400S, infrared spectra in the range of 4000–600 cm^{-1} were recorded. The ^{1}H and ^{13}C-NMR spectra were obtained with a VARIAN-INOVA 500 MHz spectrophotometer (Germany) with DMSO-d^{6} as solvent, and tetramethylsilane TMS was registered.

Methods of Preparation

Synthesis of Chalcone Derivatives [H1-H4]

Compounds [**H1-H4**] were synthesized utilizing the procedure described in the reference [28] with certain modifications. A solution of 4-amino acetophenone (0.005 mol, 0.67 g) was dissolved in 30 mL of absolute ethanol with the addition of NaOH (4 mL, 10%) and stirred at room temperature for 30 min. Substituted furan-2-carbaldehyde (0.005 mol, 1.08 g) was subsequently added and stirred for 48 h. After the disappearance of the initial components, as observed by TLC, hydrochloric acid was gradually added to the reaction mixture with stirring until a precipitate formed. This precipitate was subsequently collected through filtration, washed with cold distilled water, dried, and purified using ethyl alcohol.

(E)-1-(4-aminophenyl)-3-(5-(4-chlorophenyl) furan-2-yl) prop-2-en-1-one [H1]

Yellow powder; yield 81%; *R.f*= 7.5 (7:3, hexane: ethyl acetate); m.p: 183-185 °C; M.W: 323.78 g/mol; IR (cm^{-1}): 3429 and 3338 (NH_2), 3221 (=C-**H**), 3080 (C-H aromatic), 2956 (C-H aliphatic), 1624 (**C=O**), 1600 (-H**C=C**H-), 1560 (C=C aromatic), 822 (C-Cl). ^{1}H-NMR (500 MHz, DMSO-d_6, δ ppm): 5.10 (s, 2H, NH_2), 6.80-7.86 (m, 8H, Ar-H), 7.44-7.45 (dd, *J*=3.5 Hz, 1H, olefinic-H), 7.18-7.29 (dd, *J*=7.5 Hz, 1H, Furan-H). ^{13}C-NMR (126 MHz, DMSO-d_6, δ ppm): 188.62 (C=O), 151.29 (1C), 137.35 (1C), 132.40 (1C), 129.71 (2C), 129.10 (2C), 127.82 (1C), 127.55 (1C), 127.12 (1C), 114.23 (2C), (12C, aromatic), 154.27, 152.57, 114.44, 108.21 (4C, Furan), 127.25, 122.35 (2C, olefinic). Anal. Calcd for $C_{19}H_{14}ClNO_2$ (%): C, 70.48; H, 4.36; Cl, 10.95; N, 4.33; O, 9.88. Found: C, 70.82; H, 4.30; Cl, 10.82; N, 4.42; O, 10.20.

(E)-1-(4-aminophenyl)-3-(5-(2-nitro phenyl) furan-2-yl) prop-2-en-1-one [H2]

Orange powder; yield 85%; R.*f*= 0.66 (6:4, hexane: ethyl acetate); m.p: 150-152 °C; M.F: $C_{19}H_{14}N_2O_4$; M.W: 334.33 g/mol; IR (cm^{-1}): 3419 and 3332 (NH_2), 3217 (=C-**H**), 3043 (C-H, aromatic), 2924 (C-H, aliphatic), 1618 (**C=O**), 1597 (-H**C=C**H-), 1583 (C=C aromatic), 1531 and 1334 (NO_2), ^{1}H-NMR (500 MHz, DMSO-d_6, δ ppm): 5.41 (s, 2H, NH_2), 6.75-8.07 (m, 8H, Ar) H), 7.35-7.40 (dd, *J*=3.4 Hz, 1H, olefinic-H), 7.12-7.18 (dd, *J*=7.7 Hz, 1H, Furan-H). ^{13}C-NMR (126 MHz, DMSO-*d6*, δ ppm): 189.21 (C=O), 151.34 (1C), 146.65 (1C), 132.12 (2C), 129.82 (2C), 129.04 (1C), 128.35 (1C), 122.85 (2C), 114.44 (2C), (12C, aromatic), 153.48, 152.93, 113.82, 111.86 (4C, Furan), 126.23, 120.85 (2C, olefinic). Anal. Calcd for $C_{19}H_{14}N_2O_4$ (%): C, 68.26; H, 4.22; N, 8.38; O, 19.14. Found: C, 68.40; H, 4.11; N, 8.50; O, 19.20.

(E)-1-(4-aminophenyl)-3-(5-(2,4-dichloro phenyl) furan-2-yl) prop-2-en-1-one [H3]

Orange powder; yield 74%; R.*f*= 0.78 (8:2, hexane: ethyl acetate); m.p:188-190 °C; M.W: 358.22 g/mol; IR (cm^{-1}): 3425 and 3334 (NH_2), 3219 (=C-**H**), 3019 (C-H aromatic), 2935 (C-H aliphatic), 1614 (**C=O**), 1589 (-H**C=C**H-), 1564 (C=C aromatic) 756-833 (C-Cl), ^{1}H-NMR (500 MHz, DMSO-d_6, δ ppm): 5.46 (s, 2H, NH_2), 6.72-7.90 (m, 8H, Ar-H), 7.44-7.48 (dd, *J*=3.1 Hz, 1H, olefinic-H), 7.22-7.24 (dd, *J*=7.2 Hz, 1H, Furan-H). ^{13}C-NMR (126 MHz, DMSO-*d6*, δ ppm): 189.57 (C=O), 151.39 (1C), 137.27 (1C), 133.37 (1C), 130.57 (2C), 129.91(1C), 129.33 (2C), 127.22 (1C), 126.52 (1C), 114.79 (2C), (12C, aromatic), 152.75, 150.75, 113.78, 110.65 (4C, Furan), 125.92, 121.23 (2C, olefinic). Anal. Calcd for $C_{19}H_{13}Cl_2NO_2$; (%): C, 63.71; H, 3.66; Cl, 19.79; N, 3.91; O, 8.93. Found: C, 63.62; H, 3.82; Cl, 19.53; N, 3.97; O, 8.89.

(E)-1-(4-aminophenyl)-3-(5-(4-bromophenyl) furan -2-yl) prop-2-en-1-one [H4]

Yellow powder; yield 71%; *R.f*= 0.69 (6:4, hexane: ethyl acetate); m.p: 193-195 °C; M.W: 368.23 g/mol; IR (cm^{-1}): 3427 and 3336 (NH_2), 3223 (=C-**H**), 3030 (C-H aromatic), 2928 (C-H aliphatic), 1632 (C=O), 1589 (-H**C=C**H-), 1551 (C=C aromatic), 862 (C-Br), ^{1}H-NMR (500 MHz, DMSO-d_6, δ ppm): 5.33 (s, 2H, NH_2), 6.71-7.89 (m, 8H, Ar-H), 7.43-7.44 (dd, *J*=3.4 Hz, 1H, olefinic-H), 7.20-7.24 (dd, *J*=7.7 Hz, 1H, Furan-H). ^{13}C-NMR (126 MHz, DMSO-*d6*, δ ppm): 189.62 (C=O), 151.32 (1C), 132.93 (2C), 131.54 (1C), 129.69 (2C), 128.53 (2C), 127.93 (1C), 122.85 (1C), 114.34 (2C), (12C, aromatic), 153.90, 152.36, 112.26, 109.21 (4C, Furan), 126.52, 121.06 (2C, olefinic). Anal. Calcd for $C_{19}H_{14}BrNO_2$ (%): C, 61.97; H, 3.83; Br, 21.70; N, 3.80; O, 8.69. Found: C, 61.88; H, 3.91; Br, 21.72; N, 3.75; O, 8.66.

Synthesis of Pyrazole Derivatives [H5-H8]

A mixture of equimolar amounts of compounds [**H1-H4**] in glacial acetic acid (10 ml) and an

excess of N_2H_4. H_2O (80%, 2 ml) was refluxed for 6 h, monitored by TLC. After that, the reaction was poured into crushed ice to afford a precipitate, and the product was filtered, washed with water, dried, and crystallized from ethanol to provide compounds [**H5-H8**] [29].

_N_-(4-(1-acetyl-5-(5-(4-chlorophenyl) furan-2-yl)-4,5- dihydro-*1H*-pyrazol-3 eel) phenyl) Acetamide [H5]

Brown powder; yield 59 %; *R.f*= 0.46 (5:5, hexane: ethyl acetate); m.p: 118-120 ºC; M.W: 421.88 g/mol; IR (cm^{-1}), 3311 (N-H), 3121 (C-H, aromatic), 2925 (C-H, aliphatic), 1693 (C=O of N-C=O), 1653 (C=O of NH-C=O), 1587 (C=N), 1560 (C=C), ^{1}H-NMR (500 MHz, DMSO-d_6, δ ppm): 9.89 (s, 1H, NH), 7.80-7.40 (m, 8H, Ar-H), 6.85-6.46 (dd, 1H, *J*= 7.6, 7.5 Hz, Furan-H), 5.58 (t, 1H, *J*=6.9 Hz, pyrazole-H), 3.52-3.41 (dd, 1H, *J*= 12.4, 7.1 Hz, pyrazole-H), 2.43 (s, 3H, CH_3), 2.21 (s, 3H, CH_3). ^{13}C-NMR (126 MHz, DMSO-*d6*, δ ppm): 171.25 (C=O), 169.52 (C=O), 153.33 (C=N), 142.17 (1C), 137.66 (1C), 129.28 (2C), 128.42 (2C), 127.77 (2C), 125.16 (2C), 119.52 (2C), (12C, aromatic), 153.54, 152.21, 111.15, 108.52, (4C, Furan), 57.72 (-CH), 37.83 ($-CH_2$), 24.12 and 20.86 ($2CH_3$). Anal. Calcd for $C_{23}H_{20}ClN_3O_3$ (%): C, 65.48; H, 4.78; Cl, 8.40; N, 9.96; O, 11.38. Found: C, 65.88; H, 4.71; Cl, 8.22; N, 10.12; O, 11.30.

_N_-(4-(1-acetyl-5-(5-(2-nitrophenyl) furan-2-yl)-4,5-dihydro-*1H*-pyrazol-3-yl) phenyl) Acetamide [H6]

Yellow powder; yield 68 %; *R.f*=0.44 (5:5, hexane: ethyl acetate); m.p: 188-190 ºC; M.W: 432.44 g/mol; IR (cm^{-1}), 3331 (N-H), 3161 (C-H, aromatic), 2930 (C-H, aliphatic), 1697 (C=O of N-C=O), 1661 (C=O of NH-C=O), 1597 (C=N), 1566 (C=C), 1537-1359 (NO_2), ^{1}H-NMR (500 MHz, DMSO-d_6, δ ppm): 9.79 (s, 1H, NH), 7.98-7.62 (m, 8H, Ar-H), 6.98-6.48 (dd, 1H, *J*= 7.5, 7.6 Hz, Furan-H), 5.54 (t, 1H, *J*=6.8 Hz, pyrazole-H), 3.48-3.42 (dd, 1H, *J*= 12.2, 6.8 Hz, pyrazole-H), 2.40 (s, 3H, CH_3), 2.20 (s, 3H, CH_3). ^{13}C-NMR (126 MHz, DMSO-*d6*, δ ppm): 170.72 (C=O), 169.38 (C=O), 153.48 (C=N), 146.88 (1C), 141.38 (1C), 132.28 (1C), 129.22 (1C), 128.72 (2C), 126.75 (1C), 125.66 (1C), 123.82 (2C), 119.87 (2C), (12C, aromatic), 152.62, 151.33, 110.84, 110.32, (4C, Furan), 57.82 (-CH), 37.72 ($-CH_2$), 25.21 and 21.14 ($2CH_3$). Anal. Calcd for $C_{23}H_{20}N_4O_5$ (%): C, 63.88; H, 4.66; N, 12.96; O, 18.50. Found: C, 63.82; H, 4.68; N, 12.68; O, 18.38.

_N_-(4-(1-acetyl-5-(5-(2,4-dichlorophenyl) furan-2-yl)- 4,5-dihydro-*1H*-pyrazol-3-yl) phenyl) Acetamide [H7]

Brown powder; yield 63%; R.*f*= 0.40 (7:3, hexane: ethyl acetate); m.p:127-129 ºC; M.W: 456.32 g/mol; IR (cm^{-1}), 3311 (N-H), 3136 (C-H, aromatic), 2934 (C-H, aliphatic), 1690 (C=O of N-C=O), 1663 (C=O of NH-C=O), 1586 (C=N), 1564 (C=C), ^{1}H-NMR (500 MHz, DMSO-d_6, δ ppm): 9.72 (s, 1H, NH), 7.21-7.98 (m, 8H, Ar-H), 6.62-6.40 (dd, 1H, *J*= 7.8, 8.1 Hz, Furan-H), 5.24 (t, 1H, *J*=6.8 Hz, pyrazole-H), 3.38-3.28 (dd, 1H, *J*= 12.1, 7.2 Hz, pyrazole-H), 2.11 (s, 3H, CH_3), 2.25 (s, 3H, CH_3). ^{13}C-NMR (126 MHz, DMSO-*d6*, δ ppm): 170.82 (C=O), 169.55 (C=O), 154.28 (C=N), 141.44 (1C), 135.32 (1C), 134.11 (1C), 129.87 (2C), 128.52 (2C), 127.41 (2C), 126.32 (1C), 119.65 (2C), (12C, aromatic), 152.65, 150.38, 112.93, 109.88, (4C, Furan), 58.40 (-CH), 38.22 ($-CH_2$), 25.14 and 21.22 ($2CH_3$). Anal. Calcd for $C_{23}H_{19}Cl_2N_3O_3$ (%): C, 60.54; H, 4.20; Cl, 15.54; N, 9.21; O, 10.52. Found: C, 60.88; H, 4.08; Cl, 15.72; N, 9.32; O, 10.56.

_N_-(4-(1-acetyl-5-(5-(4bromophenyl) furan-2-yl)-4,5-dihydro-*1H*-pyrazol-3yl) phenyl) Acetamide [H8]

Brown powder; yield 61%; *R.f*= 0.67 (4:6, hexane: ethyl acetate); m.p: 107-109 ºC; M.W: 466.34; IR (cm^{-1}), 3294 (N-H), 3111 (C-H, aromatic), 2932 (C-H, aliphatic), 1696 (C=O of N-C=O), 1665 (C=O of NH-C=O), 1577 (C=N), 1564 (C=C). ^{1}H-NMR (500 MHz, DMSO-d_6, δ ppm): 9.25 (s, 1H, NH), 7.87-7.44 (m, 8H, Ar-H), 6.81-6.32 (dd, 1H, *J=7.5*, 7.7 Hz, Furan-H), 5.14 (t, 1H, *J*=6.8 Hz, pyrazole-H), 3.42-3.22 (dd, 1H, *J=12.1*, 7.2 Hz, pyrazole-H), 2.45 (s, 3H, CH_3), 2.28 (s, 3H, CH_3). ^{13}C-NMR (126 MHz, DMSO-*d6*, δ ppm): 171.37 (C=O), 168.33 (C=O), 154.28 (C=N), 142.10 (1C), 132.70 (2C), 130.48 (1C), 129.77 (2C), 128.49 (2C), 126.72 (1C), 125.33 (1C), 120.95 (2C) (12C, aromatic), 151.08, 149.87, 112.15, 109.32, (4C, Furan), 58.72 (-CH), 38.83 ($-CH_2$), 25.12 and 21.87 (2 CH_3). Anal. Calcd for $C_{23}H_{20}BrN_3O_3$ (%): C, 59.24; H, 4.32; Br, 17.13; N, 9.01; O, 10.29. Found: C, 59.18; H, 4.21; Br, 17.15; N, 8.98; O, 10.31.

In *Vitro* Antimicrobial Activity

The compounds **H5-H8** were evaluated for antibacterial activity using the disc diffusion method. Antifungal activity was measured on agar plates against the fungus Candida albicans, while antibacterial activity was assessed by in vitro culture against two Gram-positive (S. aureus and S. epidermidis) and two Gram-negative (K. pneumonia and P. aeruginosa) bacteria. [30]. The method used to propagate bacteria involved subculturing different strains of bacteria on nutrient agar for 24 h at 37°C. A Petri dish was filled with 20 mL of sterile nutritional agar. The bacterial strains' cultures were set up to grow at a McFarland value of 0.5. After the dishes were inoculated with the bacterial strains, the strains were allowed to adsorb into the gel for 15 min. Using a sterile cork borer with a 6 mm diameter, wells were created in the gel. In each well, 200 µg/mL of dimethyl sulfoxide (DMSO) was used to dissolve the test materials. The reference drug, ampicillin, was utilized at a concentration of 200 µg/mL, while the blank

(solvent) was DMSO (1 µL). The zones of inhibition have been calculated after 24 h [31, 32].

Molecular Docking

This work utilized a specific computational method. The GOLD Suite was used to perform molecular docking studies on the compounds, a completely licensed CCDC product. The following were shown using the CCDC Hermes visualizer software (version 2021.2.0): This study focuses on ligands, brief contacts, hydrogen-bonding interactions, proteins, and bond-length calculations. The chemical structures of our ligands were drawn using ChemDraw Professional [33]. The Swiss ADME server was used to predict the pharmacokinetic profile, or adsorption, distribution, metabolism, and excretion (ADME), of the molecules that were produced [25].

Preparation of Ligands and Protein Receptors

The Protein Data Bank (PDB) provided the crystal structures of the enzyme ALDH9A1 [PDB ID: 6VR6], and Swiss PDB Viewer (v. 3.7) was used to add missing atoms. To produce the correct ionization and tautomeric states of amino acid residues. The crystal structures of the protein we downloaded lacked all water molecules, and hydrogen atoms were inserted. To reduce the energy of our generated ligands, the MM2 force field has been utilized for Chem3D (v. 16.0) [34].

ADME Procedures

Swiss ADME, a tool that predicts physicochemical features and pharmacokinetic parameters by using BOILED-EGG, the polarity and lipophilicity of the small molecule were determined [35].

RESULTS AND DISCUSSION

Chemistry

The synthesis of pyrazole derivatives [**H5-H8**] was achieved through the condensation of chalcone derivatives and hydrazine hydrate in absolute ethanol, with the addition of glacial acetic acid, as illustrated in Scheme 1. Chalcones [**H1-H4**] were produced as starting materials via Claisen-Schmidt condensation using 10% NaOH, utilizing the appropriate substituted furan-2-carbaldehyde and 4-amino acetophenone in ethanol [36]. FT-IR, ^{1}H NMR, ^{13}C NMR, and elemental analysis spectrometry were used for the formation of the synthesized compounds. FT-IR spectra for chalcone derivatives [**H1-H4**] revealed the presence of bands at (3332 and 3429) cm^{-1} related to NH_2, bands at (3217 and 3223) cm^{-1} and (3019 and 3080) cm^{-1} regions due to CH=CH and C-H aromatic bands, respectively. The C=O absorption band appeared at (1614 and 1632) cm^{-1}, while the C=C stretching frequency of compounds appeared at (1551 and 1600) cm^{-1}, ^{1}H-NMR spectra showed the presence of singlet signals at (5.10-5.46) ppm due to NH_2 protons, while the multiple signals at (6.71-7.90) ppm were due to aromatic protons and two protons at (7.35-7.48) ppm of the CH=CH of chalcone. The FT-IR spectra of compounds [**H5-H8**] showed the absence of carbonyl groups of chalcone and the appearance of sharp bands at (3294 and 3331) cm^{-1} of NH groups and the stretching of two carbonyl groups at (1653 and 1665) cm^{-1} and (1690 and 1697) cm^{-1} corresponding to CH_3-CO-NH and CH_3-CO-N of the pyrazole ring, respectively. ^{1}H-NMR spectra showed a singlet signal at (9.25-9.89) ppm corresponding to NH protons, six protons for two methyl groups at (2.11-2.43) ppm, the CH_2 protons of pyrazole rings appeared as a doublet of doublets at (3.22-3.52) ppm and a triplet at (5.14-5.58) ppm. ^{13}C NMR spectra indicated the presence of –N-C=O at (170.72-171.37) ppm, NH-C=O at (168.33-169.55) ppm, and C=N at (153.33-154.28) ppm, along with signals for all other carbon atoms. The structures of [**H1-H8**] were established based on elemental analysis. All compounds assessed in molecular docking demonstrated significant activities when compared to 6VR6 as a reference drug. The compounds that were developed have been produced efficiently. The evaluation of the end products for antioxidant characteristics indicates that the new pyrazole derivatives have enhanced their antimicrobial activities. Docking studies reveal that the initial investigation of antioxidant activity demonstrates that compounds [**H5-H8**] exhibit strong antioxidant properties related to their hydrogen bonding interactions with major amino acids in ALDH9A1.

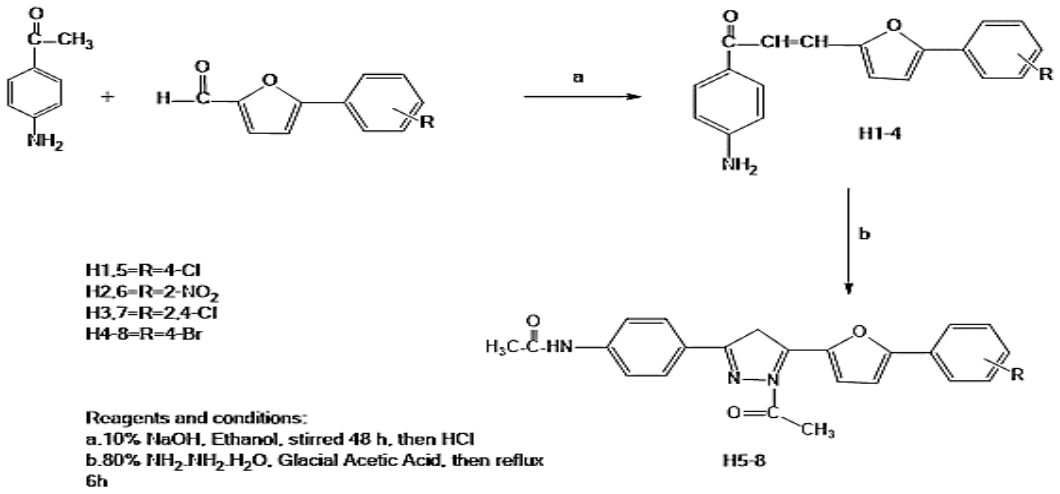

Scheme 1. Preparation Pathways of Pyrazole Derivatives.

In *Vitro* Antimicrobial Assays

Significant structural differences among [**H5-H8**] are observed in the aromatic ring, specifically at the position of the furan-2-carbaldehyde moiety. The synthetic compounds were assessed for their antibacterial and antifungal properties against Gram-positive bacteria (*S. aureus and S. epidermidis*), Gram-negative bacteria (*K. pneumonia and P. aeruginosa*), and the fungus *Candida albicans*. Compound **H5** exhibited the most significant antibacterial effect, indicating a 22 mm diameter area of inhibition. In contrast, compounds **H6-H8** displayed moderate antibacterial activity against *S. aureus*, with inhibition zone diameters varying from 9 to 17 mm. Compounds **H5-H8** exhibited moderate antibacterial activity against S. epidermidis, with inhibition zone diameters between 8 and 16 mm.

Compounds **H5-H8** exhibited moderate antibacterial activity against *P.aeruginosa*, with inhibition zone diameters between 9 and 18 mm. Compounds **H5-H8** exhibited moderate antibacterial activity against *K. pneumonia*, characterized by an inhibitory zone diameter ranging from 10 to 17 mm. The antifungal efficacy of the evaluated compounds towards *Candida albicans* demonstrated that compounds **H5** and H8 displayed moderate antifungal activity, with inhibition zones of 12.9 mm, whereas the remaining compounds exhibited no effect. Compound **H5**, containing the 4-Cl group, exhibited biological activities in the conducted studies. However, variations in other substituents significantly influenced activity, as evidenced by instances where screened chemicals showed medium efficacy against specific microbes. **Table 1** revealed the obtained results.

Table 1. The inhibition percentage of compounds **H5-H8**.

Compounds	Inhibition zone diameter (mm)				
	S.aureus	*S.epidermidis*	*P.aeruginosa*	*K.pneumonia*	*Candida albicans*
DMSO	-	-	-	-	-
H5	22	16	18	17	12
H6	9	14	9	12	-
H7	15	8	13	10	-
H8	17	12	15	14	9
Ampicillin	28	24	27	29	18

Table 2. Pyrazole derivative binding energies and reference docked.

Compounds	Binding energy (PLP Fitness)	Number of Amino acids included in H-bonding	Amino acids included in H-bonding	No. of bonding	Power of bonding
6VR6	59.82	5	GLY154	2	2.588-2.837
			TRP156	1	2.767
			THR231	1	2.671
			ARG338	1	2.746
H5	77.41	3	SER233	2	2.933-2.991
			THR236	1	2.982
H6	72.91	2	SER233	1	2.851
			GLY154	1	2.910
			TRP156	1	3.093
H7	73.77	2	ALA213	1	2.913
H8	74.48	1	LYS180	1	2.943

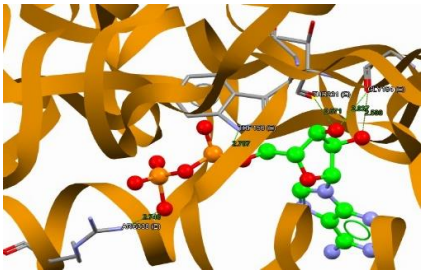

3D Structure of 6VR6

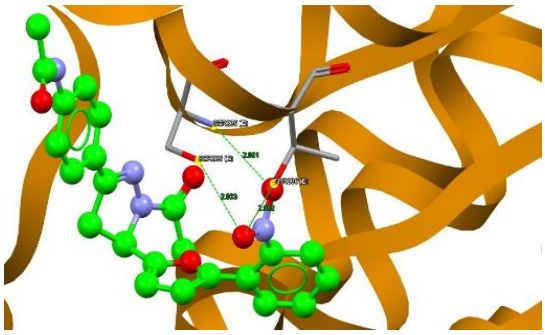

Conformer 1 of compound H5 inside the active site of the enzyme

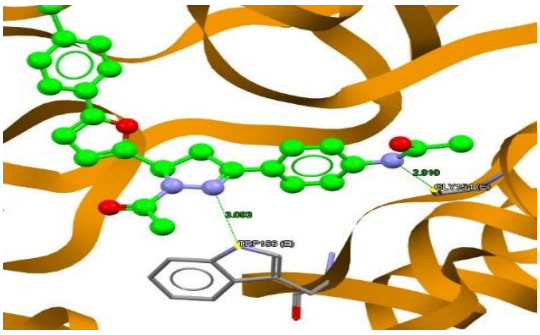

Conformer 2 of compound H6 inside the active site of the enzyme

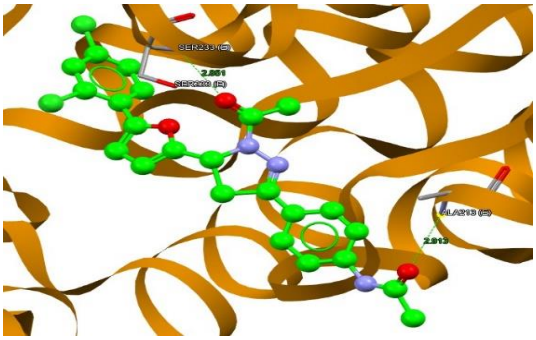

Conformer 3 of compound H7 inside the active site of the enzyme

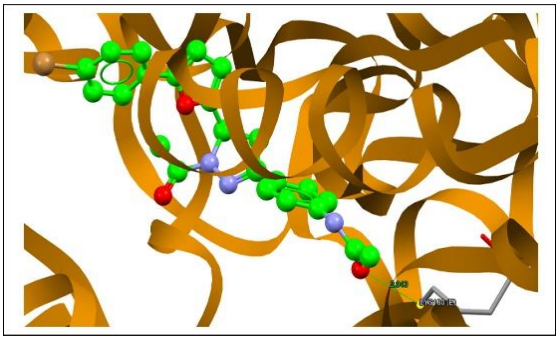

Conformer 4 of compound H8 inside the active site of the enzyme

Figure 3. Docking of the potent compounds **H5-H8** inside the binding pocket of 6VR6.

Docking Study

To study the interactions between molecules (ligands) and certain sites in the protein structure (binding), the Gold genetic algorithm for docking flexible ligands into protein binding sites [37]. The radius of the active site (10 Å) was measured using the protein's reference ligand, and has been widely validated and demonstrated great rendering for posture prediction, as well as steric complementarity between protein and ligand is calculated while the function according to CHEMPLP, the distance and angle dependent hydrogen is kept the default. All complexes are scored according to CHEMPLP fitness, with outstanding results for virtual screening [38]. The analysis of docking findings, specifically the binding mode, docked pose, and binding free energy, was conducted to assess the interactions among the molecular components associated with the active binding sites of the target protein 6VR6 and the synthesized compounds [**H5-H8],** as shown in Table 2.

GOLD measures the length of all bonds below 3 Å, including hydrogen bonds and small interactions between a particular protein atom and synthetic ligands. Additional interacting forces, including van der Waals, electrostatic, steric, p–p stacking, dipole–dipole, and others, are referred to as short contacts. The investigated compounds exhibited good levels of binding energies (72.91 to 77.41) when compared to 6VR6, which has a binding energy value of 59.82. The residues of amino acids SER233, THR236, LYS180, ALA213, GLY154, and TRP156 exhibit the best interactions. Consequently, the deactivation of the enzyme ALDH9A1 due to fitting in the active site could be the cause of the tested compound's biological action [39], as shown in Figure 3.

ADME Studies

All of the compounds are completed. The Swiss ADME server examined the profile of ADME properties of our produced compounds in order to identify the safer and promising drug candidate or candidates and to exclude those that are most likely to fail in later phases of drug development because of unfavorable ADME features.

The ADME approach has been examined for all produced substances. Additionally, as the topology polar surface area (TPSA) is another crucial factor associated with drug bioavailability, we examined it. Therefore, passively absorbed compounds are considered to have limited oral bioavailability if their TPSA is greater than 140 Å. The ADME approach has been examined for all produced substances. Additionally, as the topology polar surface area (TPSA) is another crucial factor associated with drug bioavailability, we examined it. Therefore, passively absorbed compounds are considered to have limited oral bioavailability if their TPSA exceeds 140 Å. The degree of a molecule's intestinal absorption after oral delivery is measured by the GI absorption score. If the result was high, the absorption could be excellent. All of the chemicals in this investigation had good GI absorption, which indicates that the intestines will absorb them well. The generated compounds' ADME property profiles [40] are shown in Table 3.

Table 3. The ADME properties profiles of the synthesized compounds.

Comps.	Formula	M.Wt (g/mol)	H-bond acceptors	H-bond donors	MR	TPSA Å²	GI Abs.	BBB permeant	Lipinski violations
H1	**C19H14ClNO2**	**323.77**	**2**	**1**	**93.36**	**56.23**	**High**	**Yes**	**0**
H2	**C19H14N2O4**	**334.33**	**4**	**1**	**97.18**	**102.05**	**High**	**No**	**0**
H3	**C19H13Cl2NO2**	**358.22**	**2**	**1**	**98.37**	**56.23**	**High**	**No**	**0**
H4	**C19H14BrNO2**	**368.22**	**2**	**1**	**96.05**	**56.23**	**High**	**Yes**	**0**
H5	**C23H20ClN3O3**	**421.88**	**4**	**1**	**124.06**	**74.91**	**High**	**Yes**	**0**
H6	**C23H20N4O5**	**432.43**	**6**	**1**	**127.87**	**120.73**	**High**	**No**	**0**
H7	**C23H19Cl2N3O3**	**456.32**	**4**	**1**	**129.07**	**74.91**	**High**	**No**	**0**
H8	**C23H20BrN3O3**	**466.33**	**4**	**1**	**126.75**	**74.91**	**High**	**Yes**	**0**

A series of pyrazole derivatives has been synthesized, and the identification of the resultant compounds [H1-H8] was validated using FT-IR, ^{1}H-NMR, ^{13}C-NMR, and elemental analysis. The produced compounds are regarded as promising antibacterial and antifungal agents, as demonstrated by the results of the biological activity investigations. The initial investigation of antioxidant activity revealed that compounds [H5-H8] exhibit significantly higher antioxidant effects. Molecular docking studies indicated that the potential mechanism of action involves the binding of these compounds to a specific site on the enzyme aldehyde dehydrogenase 9A1 (ALDH9A1), resulting in substantial inhibition of its activity. The ADME investigations indicated that all compounds adhered to the Lipinski rule and that all synthesized compounds were derived from the gastrointestinal tract.

ACKNOWLEDGEMENT

This study was supported by the Department of Pharmaceutical Chemistry, College of Pharmacy. Al-Nahrain University, Baghdad, Iraq.

REFERENCES

1. Kumar, G., Siva Krishna, V., Sriram, D., Jachak, S. M. (2020) Pyrazole–coumarin and pyrazole–quinoline chalcones as potential antitubercular agents. *Arch Pharm (Weinheim)*, **353(8)**.

2. Megally Abdo, N. Y., Samir, E. M., Mohareb, R. M. (2020) Synthesis and evaluation of novel 4H-pyrazole and thiophene derivatives derived from chalcone as potential anti-proliferative agents, Pim-1 kinase inhibitors, and PAINS. *J. Heterocycl Chem.*, **57(4),** 1993–2009.

3. Murwih Alidmat, M., Khairuddean, M., Mohammad Norman, N., Mohamed Asri, A. N., Mohd Suhaimi, M. H., Sharma, G. (2021) Synthesis, characterization, docking study, and biological evaluation of new chalcone, pyrazoline, and pyrimidine derivatives as potent antimalarial compounds. *Arab J. Chem.*, **14(9)**.

4. Suma, V. R., Sreenivasulu, R., Rao, B. V. M., Subramanyam, M., Ahsan, J. M., Alluri, R., Rao M. R. K. (2020) Design, synthesis, and biological evaluation of chalcone-linked thiazole-imidazopyridine derivatives as anticancer agents. *Med. Chem. Res. [Internet]*, **29(9)** 1643–1654. *Available from.*

5. Al-Saheb, R., Makharza , S., Al-Battah, F., Abu-El-Halawa, R., Kaimari, T., Abu Abed (2020) OS. Synthesis of new pyrazolone and pyrazole-based adamantyl chalcones and antimicrobial activity. *Biosci. Rep.*, **40(9)**, 1–13.

6. Shaik, A. B., Bhandare, R. R., Nissankararao, S., Edis, Z., Tangirala, N. R., Shahanaaz, S, Rahman, M. M. (2020) Antiproliferative Activities. *Molecules*, **25(3188)**, 1–16.

7. Basappa, V. C., Ramaiah, S., Penubolu, S., Kariyappa, A. K. (2022) Recent developments on the synthetic and biological applications of chalcones review. *Biointerface Res. Appl. Chem.*, **12(1)**, 180–195.

8. Mansour, E., Aboelnaga, A., Nassar, E. M., Elewa, S. I. (2020) A new series of thiazolyl pyrazoline derivatives linked to benzo[1,3]dioxole moiety: Synthesis and evaluation of antimicrobial and anti-proliferative activities. *Synth Commun.*, **50(3)**, 368–379.

9. Sahu, K. N., Balbhadra, S. S, Choudhary, J. V., Kohli, D. (2021) Exploring Pharmacological Significance of Chalcone Scaffold: A Review. *Curr. Med. Chem.*, **19(2)**, 209–225.

10. Maciejewska, N., Olszewski, M., Jurasz, J., Serocki, M., Dzierzynska, M., Cekala, K., Wieczerzak, E., Baginski, M. (2022) Novel chalcone-derived pyrazoles as potential therapeutic agents for the treatment of non-small cell lung cancer. *Sci. Rep. [Internet]*, **12(1)**, 1–19. https://doi.org/10.1038/s41598-022-07691-6.

11. Rohman, N., Ardiansah, B., Wukirsari, T., Judeh, Z. (2024) Recent Trends in the Synthesis and Bioactivity of Coumarin, Coumarin–Chalcone, and Coumarin–Triazole Molecular Hybrids. *Molecules*, **29(5)**.

12. Kasetti, A. B., Singhvi, I., Nagasuri, R., Bhandare, R. R., Shaik, A. B. (2021) Thiazole–chalcone hybrids as prospective antitubercular and anti-proliferative agents: Design, synthesis, biological, molecular docking studies, and in silico ADME evaluation. *Molecules*, **26(10)**, 1–17.

13. Salian, V. V., Narayana, B., Sarojini, B. K., Byrappa, K. (2018) A Comprehensive Review on Recent Developments in the Field of Biological Applications of Potent Pyrazolines Derived from Chalcone Precursors. *Letters in Drug Design & Discovery*, **15**, 516–574.

14. Mantzanidou, M., Pontiki, E., Hadjipavlou-Litina, D. (2021) Pyrazoles and pyrazolines as anti-inflammatory agents. *Molecules*, **26(11)**.

15. Mor, S., Khatri, M., Punia, R., Nagoria, S., Sindhu, S. (2022) A New Insight into the Synthesis and Biological Activities of Pyrazole-based Derivatives. *Mini Rev. Org. Chem.*, **19(6)**, 717–778.

16. Anil, D., Caykoylu, E. U., Sanli, F., Gambacorta, N., Karatas, O. F., Nicolotti, O., Algul, O., Burmaoglu, S. S. (2021) Synthesis and biological evaluation of 3,5-diaryl-pyrazole derivatives as potential antiprostate cancer agents. *Arch Pharm (Weinheim)*, **354(12)**, 1–9.

17. Bhirud, J. D., Gupta, G. R., Narkhede, H. P. (2020) Oxidative Cyclization of Chalcones in the Presence of Sulfamic Acid as Catalyst. Synthesis, Biological Activity, and Thermal Properties of 1,3,5-Trisubstituted Pyrazoles. *Russ. J. Org. Chem.*, **56(10)**, 1815–1822.

18. Payne, M., Bottomley, A. L., Och, A., Asmara, A. P., Harry, E. J., Ung, A. T. (2021) Synthesis and biological evaluation of 3,5-substituted pyrazoles as possible antibacterial agents. *Bioorganic Med. Chem.*, **48**.

19. Alam, M. J., Alam, O., Perwez, A., Rizvi, M. A., Naim, M. J., Naidu, V. G. M., Imran, M., Ghoneim, M. M., Alshehri, S., Shakeel, F. (2022) Design, Synthesis, Molecular Docking, and Biological Evaluation of Pyrazole Hybrid Chalcone Conjugates as Potential Anticancer Agents and Tubulin Polymerization Inhibitors. *Pharmaceuticals*, **15(3)**.

20. Tok, F., İrem Abas, B., Çevik, Ö., Koçyiğit-Kaymakçıoğlu, B. (2020) Design, synthesis and biological evaluation of some new 2-Pyrazoline derivatives as potential anticancer agents. *Bioorganic Chemistry*, **102**.

21. Taher, A. T., Mostafa Sarg, M. T., El-Sayed Ali, N. R., Hilmy Elnagdi, N. (2019) Design, synthesis, modeling studies, and biological screening of novel pyrazole derivatives as potential analgesic and anti-inflammatory agents. *Bioorg. Chem.*, **89**, April, 2019.

22. Elsherif, M. A., Hassan, A. S., Moustafa, G. O., Awad, H. M., Morsy, N. M. (2020) Antimicrobial evaluation and molecular properties prediction of pyrazolines incorporating benzofuran and pyrazole moieties. *J. Appl. Pharm. Sci.*, **10(2)**, 37–43.

23. Bhadoriya, U., Jain, D. K. (2018) Synthesis, biological evaluation, and molecular docking study of some new pyrazoline derivatives as cyclooxygenase-II inhibitors and anti-inflammatory agents. *Indian J. Heterocycl Chem.*, **28(3)**, 407–413.

24. Kisan Rasal, N., Bhaskar Sonawane, R., Vijay Jagtap, S. (2021) Synthesis, Characterization, and Biological Study of 3-Trifluoromethylpyrazole Tethered Chalcone-Pyrrole and Pyrazoline-Pyrrole Derivatives. *Chem. Biodivers.*, **18(10)**.

25. Daina, A., Michielin, O., Zoete, V. (2017) Swiss ADME: A free web tool to evaluate pharmacokinetics, drug-likeness and medicinal chemistry friendliness of small molecules. *Sci. Rep.*, **7**, 42717.

26. Macarini, A. F., Sobrinho, T. U. C., Rizzi, G. W., Corrêa, R. (2019) Pyrazole–chalcone derivatives as selective COX-2 inhibitors: design, virtual screening, and in vitro analysis. *Med. Chem. Res.*, **28(8)**, 1235–1245.

27. Ali, S. A., Awad, S. M., Said, A. M., Mahgoub, S., Taha, H., Ahmed, N. M. (2020) Design, synthesis, molecular modeling, and biological evaluation of novel 3-(2-naphthyl)-1-phenyl-1H-pyrazole derivatives as potent antioxidants and 15-Lipoxygenase inhibitors. *J. Enzyme Inhib Med. Chem. [Internet]*, **35(1)**, 847–863.

28. Abid, S., Abdula, A. M., Al Marjani, M., Abdulhameed, Q. (2019) Synthesis, antimicrobial, antioxidant, and docking study of some novel 3, 5-disubstituted-4, 5-dihydro-1H-pyrazoles incorporating imine moiety. *Egypt J. Chem.*, **62(4)**, 739–749.

29. Saleh, M., Ayoub, A. I., Hammady, A. O. (2020) Synthesis of biological studies of some new heterocyclic compounds derived from 2-chloro-3-formyl quinoline and 4-(benzyl sulfonyl) acetophenone. *Egypt J. Chem.*, **63(12)**, 4769–7476.

30. Ayrim, N. B., Balakit, A. A., Lafta, S. J. (2022) Synthesis, Characterization, Molecular Docking, and Biological Activity Studies of Hydrazones with 3,4,5-Trimethoxyphenyl Moiety. *Egypt J. Chem.*, **65(6)**, 159–169.

31. Ayrim, N. B., Hafedh, F. R., Kadhim, Y. M., Hussein, A. S., Abdula, A. M., Mohsen, G. L., Sami, M. M. (2024) Hexahydro-1,2,3-triazine Derivatives: Synthesis, Antimicrobial Evaluation, Antibiofilm Activity, and Study of Molecular Docking Against Glucosamine-6-Phosphate. *Indones. J. Chem.*, **24(1)**, 141–151.

32. Pola, S., Banoth, K. K., Sankaranarayanan, M., Ummani, R., Garlapati, A. (2020) Design, synthesis, in silico studies, and evaluation of novel chalcones and their pyrazoline derivatives for antibacterial and antitubercular activities. *Med. Chem. Res.*, **29(10)**, 1819–1835.

33. Kadhim, H. M., Kadhim, Y. M., Fawzi, H. A., Abdul Khalik, Z. M., Jawad, A. M., Ghédira, K. (2025) Bioassay-Guided Isolation and Active Compounds Identification of the AntiDiabetic Fractions of Centaurea calcitrapa Extract and the Predicted Interaction Mechanism. *Molecules*, **30(11)**, 1–24.

34. Wyatt, J. W., Korasick, D. A., Qureshi, I. A., Campbell, A. C., Gates, K. S., Tanner, J. J. (2020) Inhibition, crystal structures, and in-solution

oligomeric structure of aldehyde dehydrogenase 9A1. *Arch Biochem Biophys*., **691**, May, 2020.

35. Makani, K. K., Shareef, M. A., Rajpurohit, H. (2019) U. S. 2018.

36. Mangouda, M. M., Hussein, M. Z., El-Bordany, E. A. (2020) Design and synthesis of novel pyrazoles, pyrazolines, and pyridines from chalcone derivatives with evaluation of their in vitro anticancer activity against T-47D and UACC-257 cell lines. *Egypt J. Chem.*, **63(12)**, 5203–5218.

37. Webb, E. F., Griswold, D. E. (1984) Micro-processor-assisted plethysmograph for the measurement of mouse paw volume. *J. Pharmacol. Methods*, **12(2)**, 149–153.

38. Palm, K., Stenberg, P., Luthman, K., Artursson, P. (1997) Polar molecular surface properties predict the intestinal absorption of drugs in humans. *Pharm. Res*., **14(5)**, 568–71.

39. Verdonk, M. L., Cole, J. C., Hartshorn, M. J., Murray, C. W., Taylor, R. D. (2003) Improved protein–ligand docking using GOLD. *Proteins Struct. Funct. Bioinforma*., **52(4)**, 609–623.

40. Suralkar, A. A., Sarda, P. S., Ghaisas, M. M., Thakare, V. N., Deshpande, A. (2008) In vivo animal models for evaluation of anti-inflammatory activity. *Latest Rev*., **6(2)**.